Received 7 April 2023; revised 31 May 2023; accepted 14 June 2023. Date of publication 26 June 2023; date of current version 25 August 2023.

Digital Object Identifier 10.1109/OJCOMS.2023.3289185

Hybrid Protocols for Relay-Assisted Non-Orthogonal Multiple Access in Power Line Communications

ROOPESH RAMESH [1] (Member, IEEE), SANJEEV GURUGOPINATH [1] (Senior Member, IEEE), AND SAMI MUHAIDAT [2,3] (Senior Member, IEEE)

[1]Department of Electronics and Communication Engineering, PES University, Bengaluru 560085, India

[2]Center for Cyber-Physical Systems, Khalifa University, Abu Dhabi, UAE

[3]Department of Electrical and Computer Engineering, Khalifa University, Abu Dhabi, UAE

CORRESPONDING AUTHOR: S. MUHAIDAT (e-mail: muhaidat@ieee.org)

ABSTRACT We study the outage probability performance of hybrid protocols in relay-assisted, non-orthogonal multiple access (NOMA)-based power line communication. In particular, we consider two networks with source, relay and destination nodes, namely, cooperative relaying NOMA (CR NOMA) and single-stage NOMA (SS NOMA). We derive closed-form expressions for the outage probabilities of three hybrid relaying techniques, namely, hybrid decode- and amplify-and-forward (HDAF), incremental HDAF (IHADF) and IHDAF with maximal ratio combining (MRC) protocols. The HDAF protocol overcomes the limitations of decode-and-forward (DF) and amplify-and-forward (AF) protocols, by combining the advantages of both. In IHDAF protocol, the advantage of successful decoding at the receiver is exploited using the direct link between source and destination nodes, with the added benefit due to HDAF. Through an extensive simulation study, we (a) validate our analysis, (b) show that IHDAF-MRC outperforms IHDAF, HDAF, DF and AF, and (c) CR NOMA outperforms SS NOMA when IHDAF-MRC scheme is employed.

INDEX TERMS Cooperative relaying, hybrid relaying protocols, maximal ratio combining, non-orthogonal multiple access, power line communication.

I. INTRODUCTION

POWER line communication (PLC) is an attractive technology and has gained prominence, since it uses the existing wired infrastructure [1], which is useful in several applications, such as Internet-of-Things (IoT) and smart grids (SG). An SG enables bidirectional exchange of data, which helps in utilizing the ability to provide a wide range of services such as data transmission, data privacy, security, load management, reliability and smart metering [2], [3], [4]. To this end, the transmitter in PLC is incorporated with coupling circuits for the transmission of a modulated carrier signal over the power line, while the receiver is equipped with coupling circuit for decoding the signal [5], [6]. The key challenges in PLC channel for data transmission along with power include receiver noise, electromagnetic interference and multipath fading, which has detrimental effect on the system performance [2], [7], [8]. To combat these challenges, orthogonal frequency division multiplexing, multiple-input multiple-output, non-orthogonal multiple access (NOMA) and cooperative relaying (CR) have been proposed for PLC [9], [10], [11]. It is known that utilizing NOMA over PLC for decode-and-forward (DF) relay-assisted PLC networks provides several advantages including reduction in electromagnetic emissions, outage and enhancement of the average sum capacity and QoS across users, in contrast to orthogonal multiple access (OMA) schemes [12], [13], [14]. Cooperative communication in PLC finds several applications in fifth generation (5G) communication systems as well, since it enhances the reliability, QoS and provides wide range of coverage including last mile connectivity [4], [15], [16]. The well-known relaying schemes in PLC include amplify-and-forward (AF) and DF schemes [17], [18], [19], [20]. In the AF scheme, the signal received in a time slot is amplified and forwarded

to the receiver by the relay. On the other hand, in the DF scheme, the symbols received in a time slot at the relay are decoded and forwarded to the receiver in the next consecutive time slot. It is well-known that the DF scheme has a higher processing cost, while the AF relay suffers from noise amplification.

In recent years, NOMA has emerged as an innovative multiple access scheme for beyond 5G networks that can potentially reduce interference while increasing the device propagation performance [10], [11], [13]. In NOMA, several users are served simultaneously over the same time and frequency resources, by appropriately multiplexing the transmitted signals either in code-domain or power domain. In power-domain NOMA (PD-NOMA), the users are allocated different energy levels as per the channel gains. The far user with the least channel gain with more energy while the near user with best channel gain is assigned less energy. Signals are superimposed at the transmitter, and the receiver utilizes the successive interference cancellation (SIC) technique. Consequently, NOMA offers better spectral efficiency as compared to other OMA schemes [21]. More recently, several works on integrating NOMA with relay-assisted PLC have been proposed in the literature to exploit the advantages of NOMA. In [22], CR-based NOMA (CR NOMA) for PLC was proposed, where a source modem communicates to a destination modem through a DF relay. In the first time slot, a symbol is transmitted from the source to the two receiver modems. One of the receivers acts as a relay. In the next immediate time slot, the source sends another symbol to the receiver, and the relay forwards the symbol received in the previous time slot to the receiver. The symbol at the receiver is decoded by performing SIC. In [12], the authors proposed a single-stage NOMA (SS NOMA) for PLC, which is slightly different from CR NOMA. The operation of SS NOMA is similar to that of CR NOMA in the first time slot. However, in the immediate next time slot, the relay decodes the symbol and transmits it to the other node. The receiver decodes the symbols directly in both time slots. This idea was further investigated in [13], where a dual-stage (DS) setup was considered, which was shown to outperform the SS NOMA. More recently, the authors in [14] studied the outage probability performance of NOMA-PLC considering both SS and DS schemes. It was shown that DS-NOMA outperforms SS NOMA in terms of outage probability. Moreover, there are studies with different setups in a two-user NOMA for a hybrid wireless-PLC network [10], [23]. Additionally, it is known that the CR NOMA outperforms SS NOMA in terms of overall outage probability and average capacity [22].

In wireless communications, several hybrid relaying schemes have been proposed for performance enhancement in NOMA-based cooperative communication [24], [25], [26]. In [26], the authors demonstrated that the performance of DF-NOMA is superior to AF-NOMA. The authors in [27] proposed AF-NOMA with MRC at the destination. In [28], the authors proposed a hybrid decode- and AF (HDAF) relaying scheme for NOMA-based cooperative communication and showed that it offers better throughput than AF and DF schemes. The authors in [29] proposed a relay-assisted NOMA scheme with HDAF protocol, and showed that it achieves low latency and better system throughput in comparison with the existing multicast scheme. In [30], the authors proposed the incremental HDAF (IHDAF) scheme, where relay either chooses AF or DF to transmit data or remains silent, based on the channel gains. It was also demonstrated that the IHDAF scheme outperforms HDAF scheme, in terms of outage probability. In [31], the authors used the IHDAF scheme, based on [28], [30], and showed that it outperforms other relaying schemes, along with a study on trade-off in terms of the hardware implementation. In the incremental relaying scheme, a relay participates in the cooperative communication only when the quality of the channel from source to destination is below a given threshold, which helps in achieving a higher spectral efficiency [32], [33]. Note that the above-mentioned works are restricted to wireless networks, and do not consider PLC networks.

In this paper, motivated by the fact that the HDAF and IHDAF protocols offer a better outage performance than conventional AF and DF in NOMA-based cooperative wireless communication, we investigate the HDAF and IHDAF in NOMA-based, relay-assisted PLC networks. In particular, we study the outage probabilities of CR NOMA and SS NOMA. To the best of our knowledge, the performance of CR or SS schemes in NOMA-PLC networks for HDAF and IHDAF hybrid protocols, and their corresponding analysis and comparison of outage probabilities have not been reported in the literature so far. The major contributions of this work are listed as follows.

- We propose the HDAF, IHDAF and IHDAF with maximal ratio combining (IHDAF-MRC) protocols for relay-assisted NOMA in PLC.
- We consider the CR NOMA and SS NOMA schemes with source, relay, and destination modems. For both cases, we present an analysis on the outage probabilities of HDAF, IHDAF and IHDAF-MRC protocols.
- We validate our analysis through Monte Carlo simulations, and show that the IHDAF-MRC outperforms AF, DF, HDAF and IHDAF protocols for both CR NOMA and SS NOMA schemes, in terms of outage probabilities.
- Furthermore, we show that IHDAF-MRC under the CR NOMA scheme outperforms the IHADF-MRC in SS NOMA scheme only marginally. This should be noted in contrast to the DF relaying, where it has been established that DF-aided CR NOMA outperforms DF-aided SS NOMA significantly [22].

The remainder of the paper is organized is as follows. System models for CR NOMA and SS NOMA setups and details on the hybrid relaying schemes are discussed in Section II. Analytical expressions for the outage probabilities for HDAF, IHDAF and IHDAF-MRC at the relay and

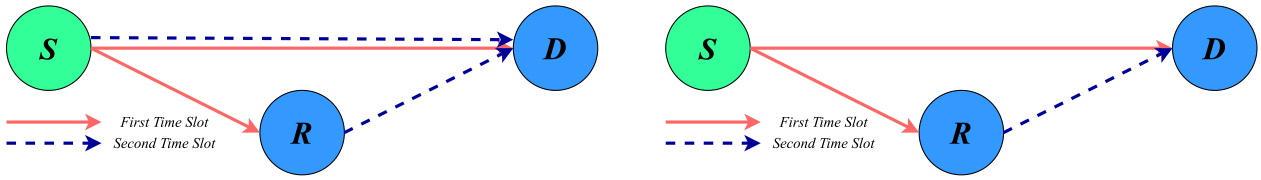

(a) CR NOMA PLC setup. (b) SS NOMA PLC setup [12]

FIGURE 1. Cooperative relay-assisted NOMA for PLC consisting of a source (S), relay (R) and destination (D) operating over two time slots, with (a) CR NOMA setup, and (b) SS NOMA setup.

TABLE 1. Table of notations.

Symbol	Description
S, R, D	Source, relay and destination modems
s_1, s_2	Symbols indented to D and R
i	Index for communication links, with $i \in \{\text{SR}, \text{SD}, \text{RD}\}$
h_i	Channel gains for link i
A_i	Attenuation factor in link i
d_i	Distance between the nodes in link i
f	Center frequency of operation
z_i	Signal received in CR NOMA scheme over link i
y_i	Signal received in SS NOMA scheme over link i
ζ_1, ζ_2	Power allocation coefficients for s_1, s_2
n_c	Additive white Gaussian noise
σ^2	Variance of n_c
Γ_i	SINR for CR NOMA scheme, due to signal received over link i
γ_i	SINR for SS NOMA scheme, due to signal received over link i
P_{out}	Outage probability at relay
P_{HDAF}	Outage probability at D for HDAF protocol
P_{IHDAF}	Outage probability at D for IHDAF protocol
$P_{\text{IHDAF-MRC}}$	Outage probability at D for IHDAF-MRC protocol
μ_i	Parameter of lognormal distribution for link i
σ_i	Parameter of lognormal distribution for link i
$\alpha_\ell \triangleq 2^{2r_\ell} - 1$	Threshold rates for outage due to symbols $\ell \in \{s_1, s_2\}$

destination nodes are derived in Section III. In Section IV, the simulation results are discussed. The concluding remarks of the paper are drawn in Section V. The notations used in this paper are given in Table 1.

II. SYSTEM MODEL

The system model, as illustrated in Fig. 1, consists of three PLC modems that operate in half-duplex mode, namely, one source (S) modem and two receiver modems. Out of the two receivers, one acts as a relay (R) and the other as the destination (D). For such a setup, two NOMA-based configurations have been proposed in the literature. These include the CR NOMA setup as shown in Fig. 1(a) [34], and the SS NOMA, which is shown in Fig. 1(b) [12]. It is important to note that in both setups, the transmission of information occurs over two-time slots. More details on these two techniques will be explained later. The channel gains for the PLC direct link S-R, S-D, and R-D are denoted by h_{SR}, h_{SD}, and h_{RD}, respectively. Further, these random variables are modeled as independent lognormal distribution random variables, which are independent and identically distributed over time [6], [35], [36]. The PDFs of h_{SR}, h_{SD} and h_{RD} are given by

$$f(h_i) = \frac{1}{\sqrt{2\pi}\sigma_i h_i} \exp\left[-\frac{(\log h_i - \mu)^2}{2\sigma^2}\right], \tag{1}$$

for $i \in \{\text{SR,SD,RD}\}$, where μ and σ^2 respectively denote the mean and the variance of $10\log_{10}(h_i)$, $i \in \{\text{SR,SD,RD}\}$. In the next two subsections, we provide details on the functionalities of CR NOMA and SS NOMA setups. Later in Section II-C, we explain the various relaying schemes considered.

A. CR NOMA SETUP

In the CR NOMA setup [34], S sends the symbol s_1 to R and D simultaneously in the first time slot. The signal at R and D are decoded directly and independently. Based on the relaying scheme chosen, R chooses to either DF or AF the received signal from the previous time slot to D in the second time slot. In addition, S sends symbol s_2 to D in the second time slot along with R. The symbol s_1 at D is decoded directly, while the symbol s_2 is decoded by performing SIC.

The signals received in the first time slot at R and D are given as

$$z_{SR} = \sqrt{P_S} s_1 h_a + n_c, \qquad a \in \{SR, SD\}, \tag{2}$$

where n_c denotes the additive white noise which is modeled as a Gaussian random variable with mean zero and variance σ^2, and P_S denotes the transmit power at S. Using (2), we calculate the signal-to-interference-plus-noise ratio (SINR) at D for decoding s_1, which is given as

$$\Gamma_{(SD,s_1)} = \rho_S A_{SD}^2(d_{SD}, f) h_{SD}^2, \tag{3}$$

where $\rho_S = \frac{P_S}{n_c}$ denotes the transmit signal-to-noise ratio (SNR). Here, $A_{SD}^2(d_{SD}, f)$ denotes the attenuation factor over the SD link, as a function of the distance between S-D, d_{SD}, and the center frequency, f [12].

B. SS NOMA SETUP

In the SS NOMA setup [12], S transmits a superimposed signal comprising of symbols s_1 and s_2 to R and D simultaneously, in the first time slot. The symbol s_1 is decoded directly at R and D, while the symbol s_2 is decoded at R by performing SIC. Depending on the chosen relaying scheme, R operates either in DF or AF mode to transmit the received signal from the previous time slot to D, in the second time slot. The symbol s_1 is then decoded directly at D. The superimposed signal sent from S to R and D is given as

$$x_S \triangleq \left(\sqrt{\zeta_1 P_S}s_1 + \sqrt{\zeta_2 P_S}s_2\right), \tag{4}$$

where ζ_1 and ζ_2 denote the power allocation coefficients for symbols s_1 and s_2 respectively, such that $\zeta_1 + \zeta_2 = 1$. The signal received at R and D can be written as

$$y_{SR} = x_S A_{SR}(d_{SR}, f)h_{SR} + n_c, \tag{5}$$
$$y_{SD} = x_S A_{SD}(d_{SD}, f)h_{SD} + n_c, \tag{6}$$

where the distance-dependent and frequency-dependent attenuations are defined as $A_i(d_i, f)$ for $i \in \{\text{SR,SD,RD}\}$, where d_{SR}, d_{SD} and d_{RD} are the distances between S-R, S-D and R-D, and f is the frequency. The SINR at D for decoding s_1 can be expressed as

$$\gamma_{(SD,s_1)} = \frac{\zeta_1 \rho_S A_{SD}^2(d_{SD}, f)h_{SD}^2}{\zeta_2 \rho_S A_{SD}^2(d_{SD}, f)h_{SD}^2 + 1}. \tag{7}$$

Towards the end of the first time slot, R employs one of the forwarding protocols discussed next, and MRC is used at D for the performance enhancement.

C. RELAYING SCHEMES

In this section, we elaborate on the relay operations considered with CR NOMA and SS NOMA setups. In particular, we present the scenarios where AF, DF, HDAF, IHDAF and IHDAF-MRC are employed at the receiver. In each case, we describe the system functionalities of CR- and SS NOMA.

1) AMPLIFY-AND-FORWARD

CR NOMA: When R chooses to amplify the received signal in the previous time slot and forward it to D in the current slot, S sends the symbol s_2 to D simultaneously. Therefore the received signal at D can be written as

$$z_{RD}^{AF} = A_{RD}(d_{RD}, f)h_{RD}\sqrt{P_R}\beta z_{SR} + A_{SD}(d_{SD}, f)h_{SD}\sqrt{P_S}s_2 + n_c, \tag{8}$$

where β is the amplification factor, given by

$$\beta = \sqrt{\frac{P_R}{A_{SR}^2(d_{SR}, f)h_{SR}^2 + \sigma^2}}. \tag{9}$$

The corresponding SINR for decoding s_1 at D can be written as (10), given at the bottom of this page. By employing the MRC at D, the total SINR for decoding s_1 can be expressed as

$$\Gamma_{(MRC)}^{AF} = \Gamma_{(SD,s_1)} + \Gamma_{(RD,s_1)}^{AF}. \tag{11}$$

SS NOMA: In SS NOMA, R forwards the signal received in the previous time slot to D, using the AF protocol in the next slot. Therefore the received signal at D is given as

$$y_{RD}^{AF} = A_{RD}(d_{RD}, f)h_{RD}\sqrt{P_R}\beta y_{SR} + n_c. \tag{12}$$

The corresponding SINR for decoding s_1 at D can be written as (13), given at bottom of this page. By employing the MRC at D, the total SINR for decoding s_1 can be expressed as

$$\gamma_{(MRC)}^{AF} = \gamma_{(SD,s_1)} + \gamma_{(RD,s_1)}^{AF}. \tag{14}$$

2) DECODE-AND-FORWARD

CR NOMA: In this case, S sends the symbol s_2 to D, while R decodes s_1 directly by considering the symbol s_2 as noise. In the same time slot, R forwards the decoded symbol s_1 to D. We assume perfect SIC at D for the ease of analysis. Hence, the symbol s_1 is decoded directly at D by considering s_2 as noise, while the symbol s_2 is decoded by performing SIC. Therefore, the signal received at D can be written as

$$z_{RD}^{DF} = A_{RD}(d_{RD}, f)h_{RD}\sqrt{P_R}s_1 + A_{SD}(d_{SD}, f)h_{SD}\sqrt{P_S}s_2 + n_c, \tag{15}$$

where P_R denotes the transmit power at R. The corresponding SINR at R for decoding s_1 can be expressed as

$$\Gamma_{(SR,s_1)}^{DF} = \rho_S A_{SR}^2(d_{SR}, f)h_{SR}^2, \tag{16}$$

and the SINR at D for decoding the symbols s_1 and s_2 can be calculated as

$$\Gamma_{(RD,s_1)}^{DF} = \frac{A_{RD}^2(d_{RD}, f)h_{RD}^2\rho_R}{A_{SD}^2(d_{SD}, f)h_{SD}^2\rho_S + 1}, \tag{17}$$

and

$$\Gamma_{(RD,s_2)}^{DF} = A_{SD}^2(d_{SD}, f)h_{SD}^2\rho_S, \tag{18}$$

$$\Gamma_{(RD,s_1)}^{AF} = \frac{\left(\rho_R\rho_S A_{SR}^2(d_{SR}, f)h_{SR}^2 A_{RD}^2(d_{RD}, f)h_{RD}^2\right)}{\left(\rho_S A_{SR}^2(d_{SR}, f)h_{SR}^2\rho_R A_{RD}^2(d_{RD}, f)h_{RD}^2\right) + \left(\rho_S A_{SR}^2(d_{SR}, f)h_{SR}^2\right) + \left(\rho_R A_{RD}^2(d_{RD}, f)h_{RD}^2\right)}. \tag{10}$$

$$\gamma_{(RD,s_1)}^{AF} = \frac{\left(\zeta_1\rho_R\rho_S A_{SR}^2(d_{SR}, f)h_{SR}^2 A_{RD}^2(d_{RD}, f)h_{RD}^2\right)}{\left(\zeta_2\rho_S A_{SR}^2(d_{SR}, f)h_{SR}^2\rho_R A_{RD}^2(d_{RD}, f)h_{RD}^2\right) + \left(\rho_S A_{SR}^2(d_{SR}, f)h_{SR}^2\right) + \left(\rho_R A_{RD}^2(d_{RD}, f)h_{RD}^2\right)}. \tag{13}$$

respectively. The transmit SNR at R is given by $\rho_R = \frac{P_R}{n_c}$. Employing MRC at D, the total SINR for decoding s_1 can be expressed as

$$\Gamma^{DF}_{(MRC)} = \Gamma_{(SD,s_1)} + \Gamma^{DF}_{(RD,s_1)}. \tag{19}$$

SS NOMA: Even in this case, R decodes the symbol s_1 directly by considering the symbol s_2 as noise, and the symbol s_2 is decoded by performing SIC. Considering perfect SIC, the SINR at R for decoding symbols s_1 and s_2 are given by

$$\gamma^{DF}_{(SR,s_1)} = \frac{\zeta_1 \rho_S A^2_{SR}(d_{SR}, f) h^2_{SR}}{\zeta_2 \rho_S A^2_{SR}(d_{SR}, f) h^2_{SR} + 1}, \tag{20}$$

and

$$\gamma^{DF}_{(SR,s_2)} = \zeta_2 \rho_S A^2_{SR}(d_{SR}, f) h^2_{SR}, \tag{21}$$

respectively. If R successfully decodes s_1 and forwards it to D, the transmitted signal from R to D is given as

$$x_R = \sqrt{P_R} s_1. \tag{22}$$

The signal received at D from R is given by

$$y^{DF}_{RD} = x_R A_{RD}(d_{RD}, f) h_{RD} x_R + n_c. \tag{23}$$

The SINR for decoding s_1 at D is expressed as

$$\gamma^{DF}_{(RD,s_1)} = \rho_R A^2_{RD}(d_{RD}, f) h^2_{RD}. \tag{24}$$

Employing MRC at D, the total SINR for decoding s_1 can be expressed as

$$\gamma^{DF}_{(MRC)} = \gamma_{(SD,s_1)} + \gamma^{DF}_{(RD,s_1)}. \tag{25}$$

3) HYBRID DECODE- AND AMPLIFY-AND-FORWARD

The DF relaying scheme does not take account into the scenario when the signal forwarded to D is not correctly decoded at R [28], [30]. In the case of wireless links, when R does not decode s_1 correctly, it has been reported that employing the HDAF protocol enhances the network performance [29]. In principle, the idea behind HDAF is to combine the advantages of AF and DF relaying schemes. Here, if the SINR at D due to the signal s_1 falls below a threshold, i.e., when $\gamma^{DF}_{(SR,s_1)} \leq \alpha_1$ for some $\alpha_1 > 0$, then AF protocol is employed. Otherwise, DF protocol is employed. A schematic representation of the working principle of HDAF protocol is described in Fig. 2.

4) INCREMENTAL HYBRID DECODE- AND AMPLIFY-AND-FORWARD

It has been established that the IHDAF protocol further improves the performance compared to the HDAF protocol, for wireless links. In the IHDAF protocol, if D fails to decode s_1 from the SD link in first time slot, i.e., when $\gamma_{(SD,s_1)} \leq \alpha_1$ for some $\alpha_1 > 0$, then R forwards it to D. Next, based on the feedback information obtained from D, S estimates whether the information has been successfully decoded by D and decides whether R needs to participate in the cooperative communication. In other words, R chooses

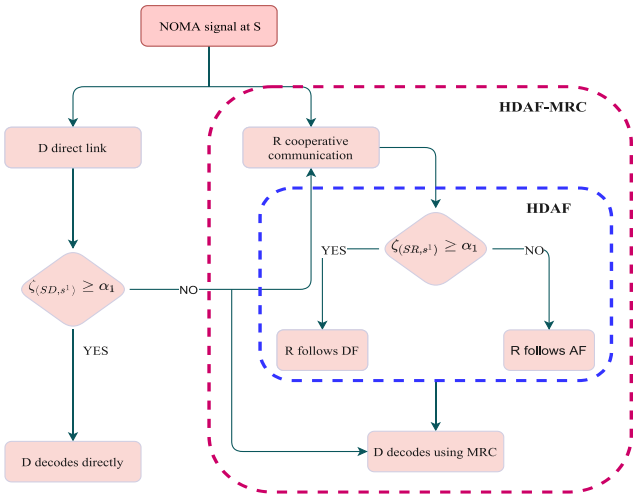

FIGURE 2. Flow of IHDAF-MRC protocol, including HDAF and IHDAF as special cases.

DF protocol only when $\gamma^{DF}_{(SR,s_1)} > \alpha_1$ and $\gamma^{DF}_{(RD,s_1)} \leq \alpha_1$, else chooses the AF protocol. In this case, R is additionally equipped for gathering the decoding consequence of SD link from S [37]. Additionally, we assume that there is perfect reception of feedback information at S [38]. A schematic representation of the working of IHDAF protocol is given in Fig. 2.

5) INCREMENTAL HYBRID DECODE- AND AMPLIFY-AND-FORWARD WITH MRC

In the first time slot in IHDAF, if D is not able to decode the symbol s_1 from the direct link, then MRC is employed at the D. This is done by combining the signal received from SD link with the signal forwarded from R in the next time slot. The benefit of employing MRC along with IHDAF protocol allows the enhancement of outage performances of both CR NOMA and SS NOMA setups. This protocol is referred to as IHDAF-MRC.

In the next section, we present an analysis on the outage probabilities for the HDAF, IHDAF and IHDAF-MRF protocols for both CR NOMA and SS NOMA schemes.

III. OUTAGE PERFORMANCE ANALYSIS

We present the mathematical analysis for the outage probabilities for symbols s_1 and s_2 at R, for symbol s_1 at D. α_1 and α_2 are the threshold rate for symbols s_1 and s_2 respectively, at both R and D.

A. OUTAGE PROBABILITY AT R

In this subsection, we derive the outage probabilities at R for CR NOMA and SS NOMA setups. First, consider CR NOMA. The outage probability for symbol s_1 at R in this case happens when it fails to decode the symbol s_1 over SR link. Therefore, the outage probability for the s_1 at R is given as [22]

$$P^{CR}_{\text{out}} \triangleq Pr\left\{\Gamma^{DF}_{(SR,s_1)} \leq \alpha_1\right\}, \tag{26}$$

$$P_{\text{out}}^{CR} = Pr\Big\{\rho_S A_{SR}^2(d_{SR},f)h_{SR}^2 \le \alpha_1\Big\}. \tag{27}$$

Following the lognormal properties 1)-3) discussed in Appendix A, an expression for the approximate outage probability at R is given as

$$P_{\text{out}}^{CR} = \frac{1}{2}\text{erfc}\left(-\frac{\log(\alpha_1) - \big(2\mu + \log\big(\rho_S A_{SR}^2(d_{SR},f)\big)\big)}{\sqrt{8}\sigma}\right), \tag{28}$$

where the complementary error function is represented by erfc(·). Next, we consider SS NOMA. The outage probability for symbols s_1 and s_2 at R for the SS NOMA occurs when it fails to decode either of the symbols over SR link. Therefore, the outage probability for both symbols at R, evaluated by using the properties 1)-3) of a lognormal distribution mentioned in Appendix A, can be written as [14]

$$P_{\text{out}}^{SS} \triangleq Pr\Big\{\gamma_{(SR,s_1)}^{DF} \le \alpha_1 \text{ or } \gamma_{(SR,s_2)}^{DF} \le \alpha_2\Big\}, \tag{29}$$

$$P_{\text{out}}^{SS} = \frac{1}{2}\text{erfc}\left(-\frac{\log(\mathcal{A}) - \big(2\mu + \log\big(\rho_S A_{SR}^2(d_{SR},f)\big)\big)}{\sqrt{8}\sigma}\right), \tag{30}$$

where $\mathcal{A} = max(\alpha_1, \alpha_2)$. In the next two subsections, we derive the overall outage probabilities at D for CR NOMA and SS NOMA setups, which is due to the symbol s_1.

For a given outage probability P_{out}, recall that the achievable diversity order is defined as

$$\mathcal{D} = \lim_{\rho\to\infty} -\frac{\log P_{\text{out}}}{\log \rho}. \tag{31}$$

From (30), using high SNR approximation on the erfc(·) function, it is easy to show that the diversity order for P_{out}^{SS} is 1, similar to the discussion in [31].

B. CR NOMA SETUP

The following Propositions 1, 2 and 3 give the approximate expressions for the overall outage probabilities at D using HDAF, IHDAF and IHDAF-MRC protocols, respectively.

Proposition 1: The approximate outage probability at D which uses the HDAF protocol due to the symbol s_1 can be written as (33), given in the bottom of this page.

Proof: See Appendix A. ■

In this case, observe that it is hard to analytically obtain the exact diversity order at the destination node under HDAF protocol, due to the complicated form of outage probability in Prop. 1.

Proposition 2: The approximate outage probability at D which uses the IHDAF protocol due to the symbol s_1 can be written as (35), given in the bottom of the page.

Proof: See Appendix B. ■

In the case of IHDAF protocol, even though analytical expression for diversity order at the destination node is hard to obtain, it is expected to be higher than 1 [31], which is later verified in Fig. 13.

Proposition 3: The approximate outage probability at D which uses the IHDAF-MRC protocol due to the symbol s_1 can be written as (37), given in the bottom of the next page.

Proof: The proof is similar to that of Proposition 1 given in Appendix A, and the corresponding mathematical details are skipped for brevity. Additionally, note that the CDF $Pr\{\Gamma_{(SD,s_1)} \le \alpha_1\}$ is calculated following the properties 1)-3) of a lognormal distribution mentioned in Appendix A. ■

The diversity order at the destination node for IHDAF-MRC protocol is known to be 2 [31].

$$P_{\text{HDAF}}^{(CR)} \triangleq Pr\Big\{\Gamma_{(SR,s_1)}^{DF} > \alpha_1, \Gamma_{(MRC)}^{DF} \le \alpha_1\Big\} + Pr\Big\{\Gamma_{(SR,s_1)}^{DF} \le \alpha_1, \Gamma_{(MRC)}^{AF} \le \alpha_1\Big\}. \tag{32}$$

$$\approx \left(\frac{1}{2}\left[\text{Q}\left(\frac{\ln(\alpha_1) + (\mu_{(SR,s_1)}^{(CR)})}{(\sigma_{(SR,s_1)}^{(CR)})}\right)\text{erfc}\left(\frac{-\ln(\alpha_1) + (\mu_{(DF,MRC)}^{CR})}{\sqrt{2}(\sigma_{(DF,MRC)}^{CR})}\right)\right] + \frac{1}{4}\left[\text{erfc}\left(\frac{-\ln(\alpha_1) + (\mu_{(SR,s_1)}^{(CR)})}{\sqrt{2}(\sigma_{(SR,s_1)}^{(CR)})}\right)\text{erfc}\left(\frac{-\ln(\alpha_1) + (\mu_{(AF,MRC)}^{CR})}{\sqrt{2}(\sigma_{(AF,MRC)}^{CR})}\right)\right]\right). \tag{33}$$

$$P_{\text{IHDAF}}^{(CR)} \triangleq Pr\{\Gamma_{(SD,s_1)} \le \alpha_1\}\Big(Pr\Big\{\Gamma_{(SD,s_1)} \le \alpha_1, \Gamma_{(SR,s_1)}^{DF} > \alpha_1, \Gamma_{(RD,s_1)}^{DF} \le \alpha_1\Big\} + Pr\Big\{\Gamma_{(SD,s_1)} \le \alpha_1, \Gamma_{(SR,s_1)}^{DF} \le \alpha_1, \Gamma_{(RD,s_1)}^{AF} \le \alpha_1\Big\}\Big). \tag{34}$$

$$\approx \left(\frac{1}{4}\left[\text{erfc}\left(\frac{-\ln(\alpha_1) + (\mu_{(SD,s_1)}^{CR})}{\sqrt{2}(\sigma_{(SD,s_1)}^{CR})}\right)\text{Q}\left(\frac{\ln(\alpha_1) + (\mu_{(SR,s_1)}^{(CR)})}{(\sigma_{(SR,s_1)}^{(CR)})}\right)\text{erfc}\left(\frac{-\ln(\alpha_1) + (\mu_{(RD,s_1)}^{(DF,CR)})}{\sqrt{2}(\sigma_{(RD,s_1)}^{(DF,CR)})}\right)\right] \times \left\{\frac{1}{2}\text{erfc}\left(-\frac{\ln(\alpha_1) + (\mu_{(SD,s_1)}^{CR})}{\sqrt{2}(\sigma_{(SD,s_1)}^{CR})}\right)\right\} + \frac{1}{8}\left[\text{erfc}\left(\frac{-\ln(\alpha_1) + (\mu_{(SD,s_1)}^{CR})}{\sqrt{2}(\sigma_{(SD,s_1)}^{CR})}\right)\text{erfc}\left(\frac{-\ln(\alpha_1) + (\mu_{(SR,s_1)}^{(CR)})}{\sqrt{2}(\sigma_{(SR,s_1)}^{(CR)})}\right)\text{erfc}\left(\frac{-\ln(\alpha_1) + (\mu_{(RD,s_1)}^{(AF,CR)})}{\sqrt{2}(\sigma_{(RD,s_1)}^{(AF,CR)})}\right)\right]\right). \tag{35}$$

C. SS NOMA SETUP

The following Propositions 4, 5 and 6 give the approximate expressions for the overall outage probabilities at D using HDAF, IHDAF and IHDAF-MRC protocols, respectively, for the SS NOMA setup. The proofs in this case are similar to the proofs in CR NOMA setup, and are skipped.

Proposition 4: The approximate outage probability at D which uses the HDAF protocol due to the symbol s_1 can be written as (39), given in the bottom of the page.

Proposition 5: The approximate outage probability at D which uses the IHDAF protocol due to the symbol s_1 can be written as (41), given at the bottom of the page.

Proposition 6: The approximate outage probability at D which uses the IHDAF-MRC protocol due to the symbol s_1 can be written as (43), given at the bottom of the page.

Even for the SS NOMA case, it is hard to obtain the diversity order at the destination node for HDAF analytically, and is straightforward to verify that the diversity order at the destination for IHDAF and IHDAF-MRC protocols are 1 and 2, respectively. This will be later verified in Fig. 14.

IV. RESULTS AND DISCUSSION

In this section, we evaluate the outage performance of our considered relay-assisted NOMA networks and validate our expressions using Monte Carlo simulations. In particular, we first discuss the results corresponding to the CR NOMA setup, followed by the SS NOMA setup. Later, we present a performance comparison of all the hybrid protocols across both setups. Unless otherwise mentioned, the parameters considered for this study are chosen from Table 2 [12], [13], [33]. The attenuation model is chosen as $A_i(d_i, f) = \exp(-\beta d_i)$, for $i \in \{\text{SR, SD, RD}\}$.

$$P^{(CR)}_{\text{IHDAF-MRC}} \triangleq Pr\left\{\Gamma_{(SD,s_1)} \leq \alpha_1\right\}\left(Pr\left\{\Gamma^{DF}_{(SR,s_1)} > \alpha_1, \Gamma^{DF}_{(MRC)} \leq \alpha_1\right\} + Pr\left\{\Gamma^{DF}_{(SR,s_1)} \leq \alpha_1, \Gamma^{AF}_{(MRC)} \leq \alpha_1\right\}\right). \tag{36}$$

$$\approx \left\{\frac{1}{2}\text{erfc}\left(-\frac{\ln(\alpha_1) + (\mu^{CR}_{(SD,s_1)})}{\sqrt{2}(\sigma^{CR}_{(SD,s_1)})}\right)\right\} P^{(CR)}_{\text{HDAF}}. \tag{37}$$

$$P^{(SS)}_{\text{HDAF}} \triangleq Pr\left\{\gamma^{DF}_{(SR,s_1)} > \alpha_1, \gamma^{DF}_{(MRC)} \leq \alpha_1\right\} + Pr\left\{\gamma^{DF}_{(SR,s_1)} \leq \alpha_1, \gamma^{AF}_{(MRC)} \leq \alpha_1\right\}. \tag{38}$$

$$\approx \left(\frac{1}{2}\left[\text{Q}\left(\frac{\ln(\alpha_1) + (\mu^{(SS)}_{(SR,s_1)})}{(\sigma^{SS}_{(SD,s_1)})}\right)\text{erfc}\left(\frac{-\ln(\alpha_1) + (\mu^{SS}_{(DF,MRC)})}{\sqrt{2}(\sigma^{SS}_{(DF,MRC)})}\right)\right] + \frac{1}{4}\left[\text{erfc}\left(\frac{-\ln(\alpha_1) + (\mu^{(SS)}_{(SR,s_1)})}{\sqrt{2}(\sigma^{(SS)}_{(SR,s_1)})}\right)\text{erfc}\left(\frac{-\ln(\alpha_1) + (\mu^{SS}_{(AF,MRC)})}{\sqrt{2}(\sigma^{SS}_{(AF,MRC)})}\right)\right]\right). \tag{39}$$

$$P^{(SS)}_{\text{IHDAF}} \triangleq Pr\left\{\gamma_{(SD,s_1)} \leq \alpha_1\right\}\left(Pr\left\{\gamma_{(SD,s_1)} \leq \alpha_1, \gamma^{DF}_{(SR,s_1)} > \alpha_1, \gamma^{DF}_{(RD,s_1)} \leq \alpha_1\right\} + Pr\left\{\gamma_{(SD,s_1)} \leq \alpha_1, \gamma^{DF}_{(SR,s_1)} \leq \alpha_1, \gamma^{AF}_{(RD,s_1)} \leq \alpha_1\right\}\right). \tag{40}$$

$$\approx \left(\frac{1}{4}\left[\text{erfc}\left(\frac{-\ln(\alpha_1) + (\mu^{SS}_{(SD,s_1)})}{\sqrt{2}(\sigma^{SS}_{(SD,s_1)})}\right)\text{Q}\left(\frac{\ln(\alpha_1) + (\mu^{(SS)}_{(SR,s_1)})}{(\sigma^{(SS)}_{(SR,s_1)})}\right)\text{erfc}\left(\frac{-\ln(\alpha_1) + (\mu^{(DF,SS)}_{(RD,s_1)})}{\sqrt{2}(\sigma^{(DF,SS)}_{(RD,s_1)})}\right)\right] \times \left\{\frac{1}{2}\text{erfc}\left(-\frac{\ln(\alpha_1) + (\mu^{SS}_{(SD,s_1)})}{\sqrt{2}(\sigma^{SS}_{(SD,s_1)})}\right)\right\} + \frac{1}{8}\left[\text{erfc}\left(\frac{-\ln(\alpha_1) + (\mu^{SS}_{(SD,s_1)})}{\sqrt{2}(\sigma^{SS}_{(SD,s_1)})}\right)\text{erfc}\left(\frac{-\ln(\alpha_1) + (\mu^{(SS)}_{(SR,s_1)})}{\sqrt{2}(\sigma^{(SS)}_{(SR,s_1)})}\right)\text{erfc}\left(\frac{-\ln(\alpha_1) + (\mu^{(AF,SS)}_{(RD,s_1)})}{\sqrt{2}(\sigma^{(AF,SS)}_{(RD,s_1)})}\right)\right]\right). \tag{41}$$

$$P^{(SS)}_{\text{IHDAF-MRC}} \triangleq Pr\left\{\gamma_{(SD,s_1)} \leq \alpha_1\right\}\left(Pr\left\{\gamma^{DF}_{(SR,s_1)} > \alpha_1, \gamma^{DF}_{(MRC)} \leq \alpha_1\right\} + Pr\left\{\gamma^{DF}_{(SR,s_1)} \leq \alpha_1, \gamma^{AF}_{(MRC)} \leq \alpha_1\right\}\right). \tag{42}$$

$$\approx \left\{\frac{1}{2}\text{erfc}\left(-\frac{\ln(\alpha_1) + (\mu^{SS}_{(SD,s_1)})}{\sqrt{2}(\sigma^{SS}_{(SD,s_1)})}\right)\right\} P^{(SS)}_{\text{HDAF}}. \tag{43}$$

TABLE 2. Parameters chosen for our Monte Carlo study.

Parameter	Value
β	$a_0 + a_1 f^r$
f	30 MHz
r	0.7
a_0	9.4×10^{-3}
a_1	4.2×10^{-7}
ζ_1	0.9
μ	0.4
σ	0.6
d_{SD}	300 m
d_{SR}	$(1/3)d_{SD}$

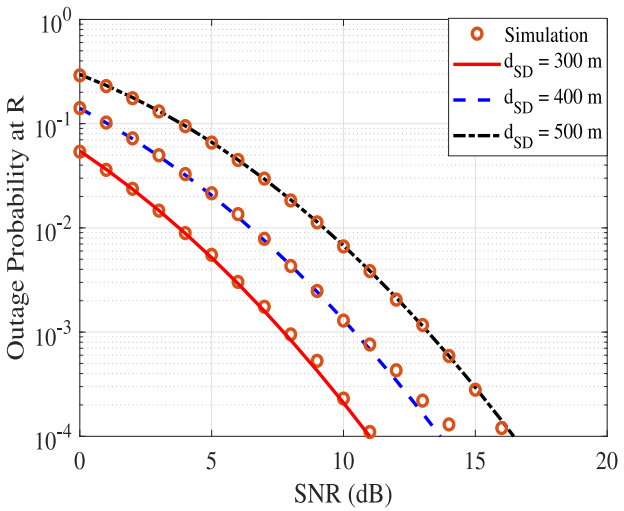

FIGURE 3. Outage at R with respect to different transmit SNR for the CR NOMA setup.

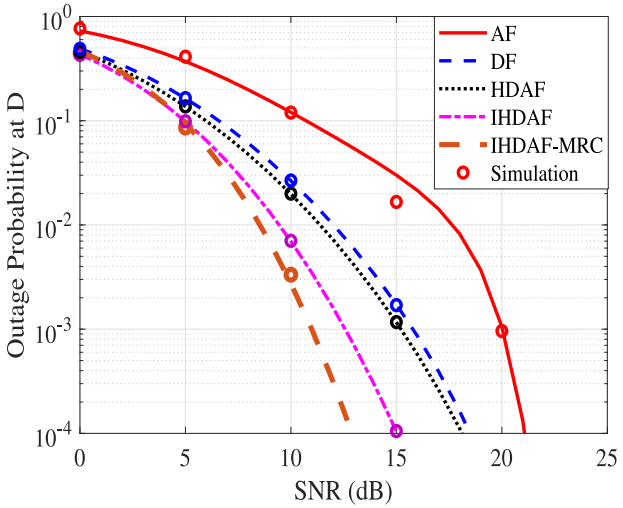

FIGURE 4. Comparison of outage at D for different forwarding protocols with respect to transmit SNR for the CR NOMA setup.

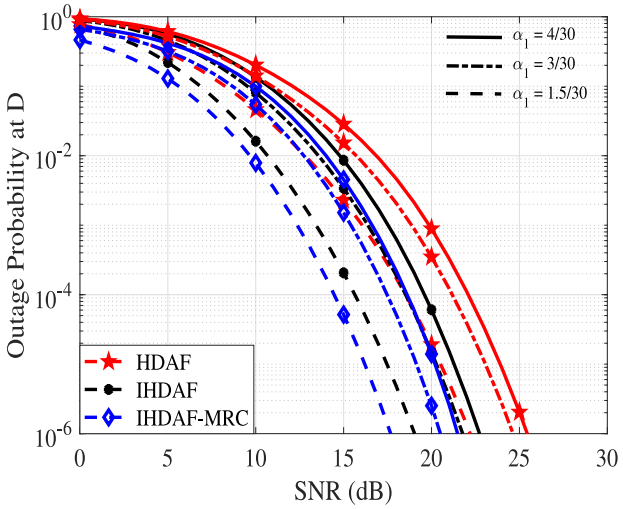

FIGURE 5. Comparison of outage at D for HDAF, IHDAF and IHDAF-MRC with respect to transmit SNR for the CR NOMA setup.

A. CR NOMA SETUP

We first consider the CR NOMA setup. Fig. 3 presents the variation in outage probability at R with respect to the transmit SNR, for different values of d_{SD}. The markers denote the set of curves obtained due to Monte Carlo simulations. To note, as d_{SD} increases, the outage probability increases due to the fact that the attenuation of the signal increases with an increase in distance. Further, a good agreement between analysis and Monte Carlo simulations can be observed. The outage at R is independent of the choice of the forwarding protocol. Fig. 4 presents the variation in outage probability at D for s_1 with respect to transmitting SNR, across all the hybrid forwarding protocols considered. In each case, it is observed that there exists a close match between our analysis and simulations. Further, it is noted that AF offers the least performance, while IHDAF-MRC performs the best. Fig. 5 presents the outage probability of D with varying threshold rates α_1 with respect to transmit SNR. The earlier set of conclusions hold even in this case. As expected, HDAF performs better than DF as the R switches between the AF and DF when the SINR at D is greater than α_1, thereby the outage performance increases marginally as opposed to just DF or the AF protocols. Fig. 6 presents a comparison of the outage probabilities at D for OMA, DF-NOMA and IHDAF-MRC schemes for the CR NOMA setup. It is seen that the performance improvement of IHDAF-MRC over OMA is about 5 dB, for a given outage probability. Additionally, as expected, the IHDAF-MRC scheme outperforms the other schemes across all SNR values. In IHDAF-MRC, along with HDAF, D employs MRC for decoding the signal from the S-D link even with a failure from AF or DF forwarding protocol. Therefore, it is observed as IHDAF-MRC performs outperforms all others.

B. SS NOMA SETUP

Next, we consider the SS NOMA setup. Fig. 7 presents the variation in outage probability at the relay with respect to transmitting SNR. Fig. 8 presents the variation in outage probability at the destination for the symbol s_1 with

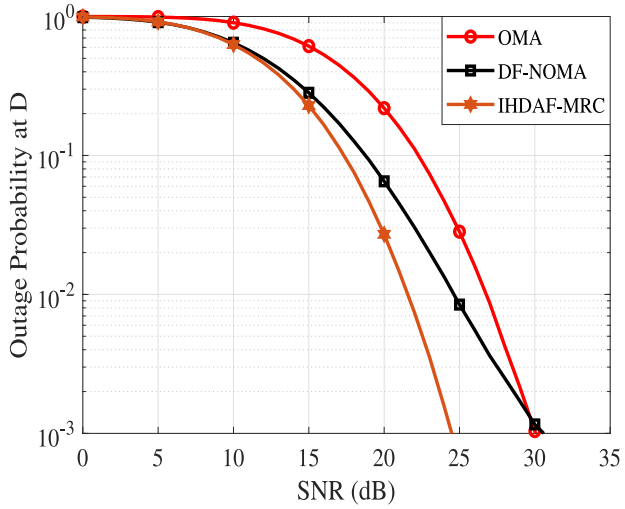

FIGURE 6. Comparison of outage at D for OMA, DF-NOMA and IHDAF-MRC with respect to transmit SNR for the CR NOMA setup.

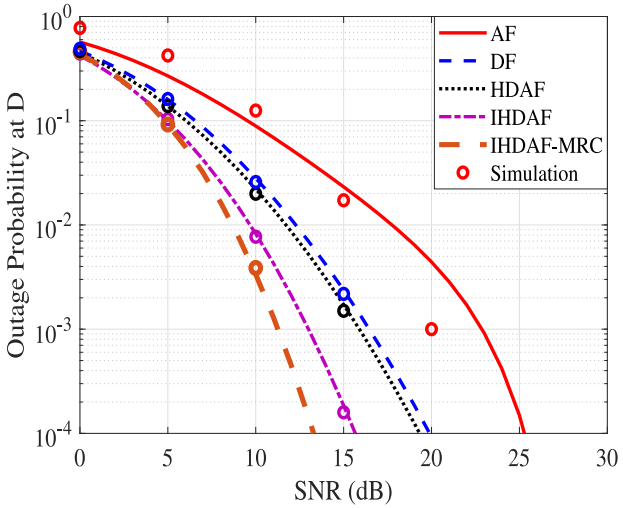

FIGURE 8. Comparison of the outage at D for different forwarding protocols with respect to transmitting SNR for the SS NOMA setup.

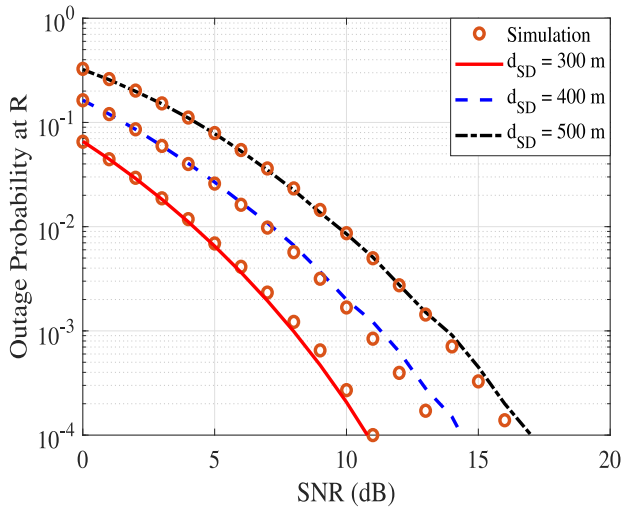

FIGURE 7. Outage at R with respect to different transmit SNR for the SS NOMA setup.

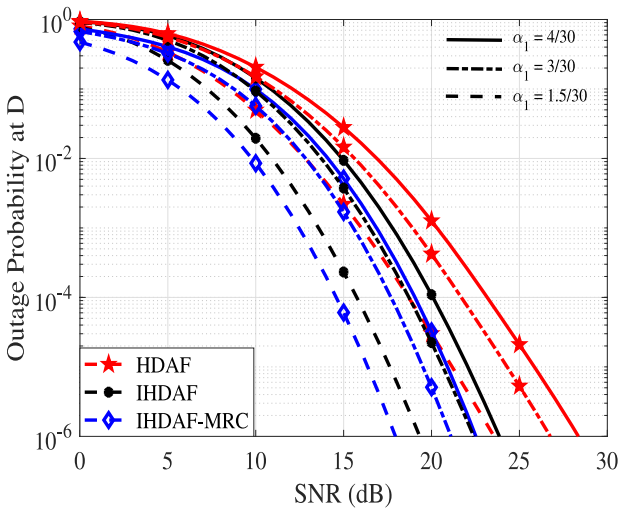

FIGURE 9. Comparison of the outage at D for HDAF, IHDAF and IHDAF-MRC with respect to transmitting SNR for the SS NOMA setup.

respect to transmit SNR. The good fit between the analytical expressions and the Monte Carlo simulation establishes the accuracy of our analysis. Fig. 9 presents the outage probability of D with varying threshold rate α_1 with respect to transmit SNR. Fig. 10 presents a comparison of the outage probabilities at D for OMA, DF-NOMA and IHDAF-MRC schemes for the SS NOMA setup. Even in this case, it is seen that the performance improvement of IHDAF-MRC over OMA is about 5 dB, for a given outage probability. Similar to CR NOMA, the IHDAF-MRC scheme outperforms the other schemes across all SNR values even in this case. The trends in these figures are similar to those obtained from the CR NOMA setup, leading to similar conclusions. It can be noted that for both setups considered in this work, IHDAF-MRC performs better than the rest. Additionally, the hardware complexity for employing IHDAF-MRC is more as compared to IHDAF.

C. PERFORMANCE COMPARISON OF CR NOMA AND SS NOMA

In this subsection, we compare the outage performances of both CR- and SS NOMA. Since IHDAF-MRC protocol was observed to offer the best performance among all the other hybrid protocols, we consider the variation in the outage probability of IHDAF-MRC at D for both setups in Fig. 11, in terms of d_{SD}. It is interesting to note that the performance of both CR- and SS NOMA setups are almost similar, with CR NOMA slightly outperforming SS NOMA. This behaviour can be seen in contrast to the comparison observed in Fig. 12, which presents the variation in the overall outage probability of both setups with the S-D distance, for different transmit SNR values using the DF scheme. Note that the CR NOMA outperforms the SS NOMA considerably. Moreover, as the distance between R-D decreases, this performance improvement is significant. Therefore, it can be

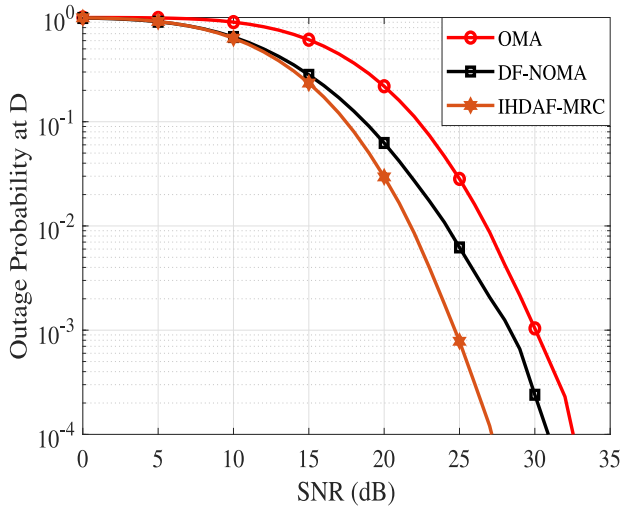

FIGURE 10. Comparison of the outage at D for OMA, DF-NOMA and IHDAF-MRC with respect to transmitting SNR for the SS NOMA setup.

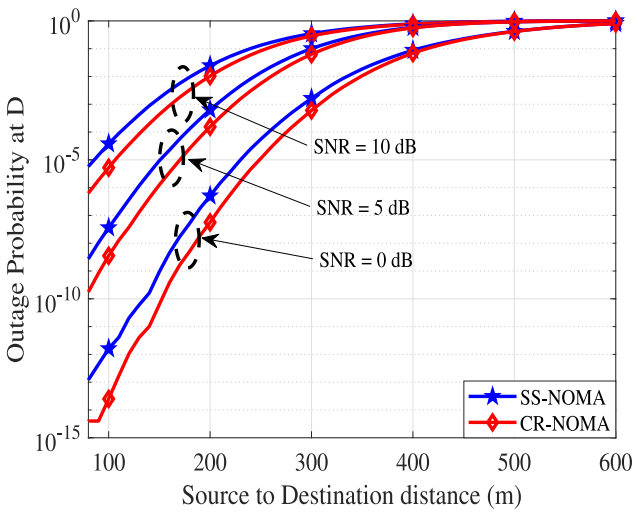

FIGURE 11. Comparison of outage probability at D for CR NOMA and SS NOMA, using IHDAF-MRC protocol.

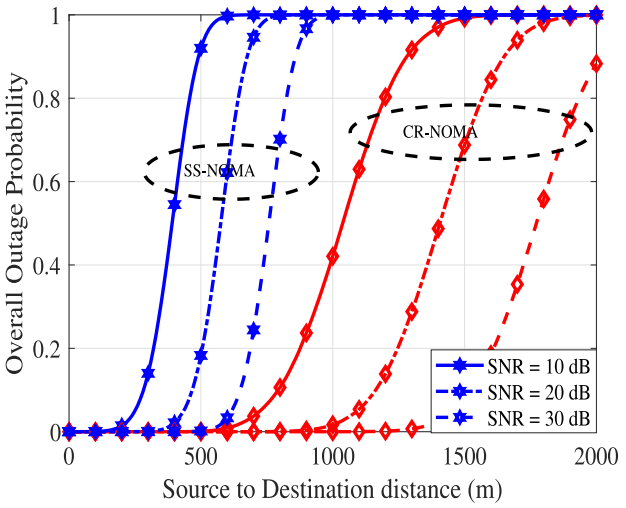

FIGURE 12. Comparison of overall outage probability for CR NOMA and SS NOMA, using DF protocol.

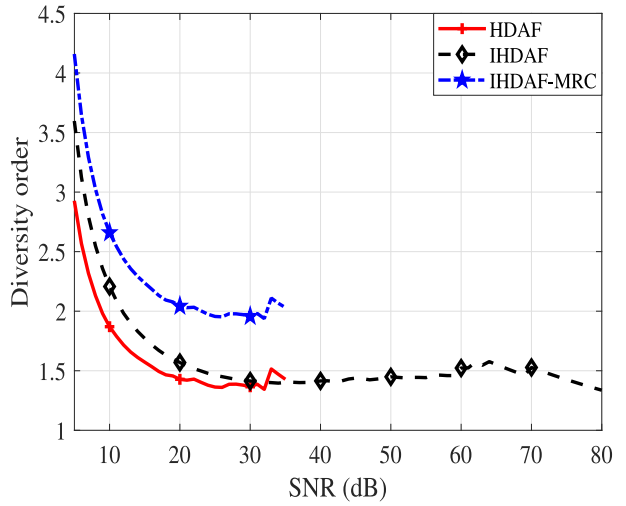

FIGURE 13. Diversity order for CR NOMA, using HDAF, IHDAF, and IHDAF-MRC protocols. Here, $\mu = 1, \sigma = 2$.

concluded that even though employing CR NOMA results in a significantly better overall outage with DF relaying in comparison with SS NOMA, the outage performance of the two are nearly equal when IHDAF-MRC protocol is employed.

Figs. 13 and 14 present a comparison of the achievable diversity orders at D for HDAF, IHDAF and IHDAF-MRC schemes for the CR NOMA and SS NOMA setups, respectively. It is observed that as the transmit SNR (ρ) approaches ∞, the IHDAF-MRC scheme can achieve a diversity order of 2, since D uses the direct link to decode its own signal by treating IHDAF as a remedial solution.

V. CONCLUSION

We presented a study on outage probability performance of hybrid relaying protocols for NOMA-based PLC networks. We considered HDAF, IHDAF and IHDAF-MRC protocols, and derived expressions for their corresponding approximate outage probabilities, using simple approximations on lognormal distribution. Two known PLC network configurations, namely, CR NOMA and SS NOMA were considered. Our Monte Carlo simulation study showed that the approximations used in our derivations are tight, and IHDAF-MRC outperforms IHDAF, HDAF, DF and AF schemes. Moreover, it was shown that CR NOMA setup marginally outperforms SS NOMA setup when IHDAF-MRC scheme is employed, while the performance improvement is significant under DF relaying.

APPENDIX A
PROOF OF PROPOSITION 1

The outage for the symbol s_1 at D occurs when D fails to decode the symbol s_1 from either SD or RD links. Therefore,

$$P_{\text{HDAF}}^{(CR)} \triangleq Pr\left\{\Gamma_{(SD,s_1)} > \alpha_1, \Gamma_{(MRC)}^{DF} \leq \alpha_1\right\} + Pr\left\{\Gamma_{(SD,s_1)} \leq \alpha_1, \Gamma_{(MRC)}^{AF} \leq \alpha_1\right\},$$

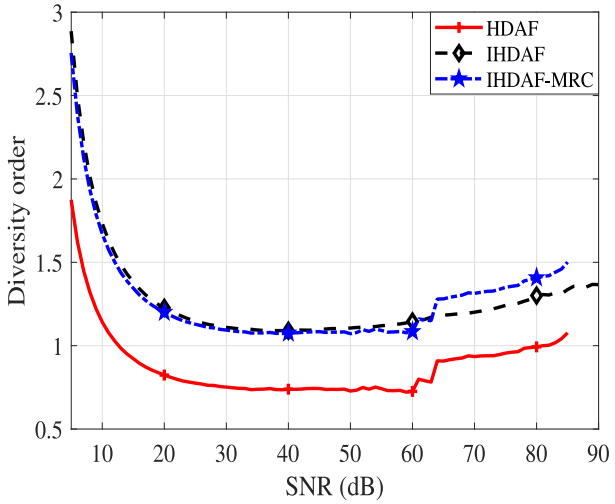

FIGURE 14. Diversity order for SS NOMA, using HDAF, IHDAF, and IHDAF-MRC protocols. Here, $\mu = 1, \sigma = 3$.

$$= \Bigg(\underbrace{Pr\{\Gamma_{(SD,s_1)} > \alpha_1\}}_{\mathcal{B}}, \underbrace{Pr\Big\{\Gamma^{DF}_{(MRC)} \leq \alpha_1\Big\}}_{\mathcal{C}} + \underbrace{Pr\{\Gamma_{(SD,s_1)} \leq \alpha_1\}}_{\mathcal{D}}, \underbrace{Pr\Big\{\Gamma^{AF}_{(MRC)} \leq \alpha_1\Big\}}_{\mathcal{E}} \Bigg). \quad (44)$$

We start by considering $\mathcal{D}$. The cumulative distribution function (CDF) of the received SINR at D is given by

$$F_{\Gamma_{(SD,s_1)}}(y) = Pr\big(\rho_S A^2_{SD}(d_{SD}, f) h^2_{SD} \leq y\big), \quad (45)$$

where, following the properties of a lognormal distribution, it is easy to see that $h^2_{SR} \sim \mathcal{LN}(2\mu^{CR}_{(SD,s_1)}, 4\sigma^{CR}_{(SD,s_1)})$. Now, recall that if $H_i \sim \mathcal{LN}(\mu_i, \sigma_i^2)$ and $H_j \sim \mathcal{LN}(\mu_j, \sigma_j^2)$, then

1) $kH_i \sim \mathcal{LN}(\mu_i + \ln k, \sigma_i^2)$, for $k \in \mathbb{R}^+$,
2) $\frac{H_i}{H_j} \sim \mathcal{LN}(\mu_l, \sigma_l^2)$; $\mu_l = \mu_i - \mu_j$, and $\sigma_l = \sigma_i + \sigma_j$,
3) $H_l = H_i + H_j$ is closely estimated as another lognormal distribution, with parameters μ_l and σ_l^2, which can be calculated as [39],

$$\mu_l = \frac{1}{2} \log \mathbb{E}\Big[H_l^{-2}\Big] - 2 \log \mathbb{E}\Big[H_l^{-1}\Big], \quad (46)$$

$$\sigma_l^2 = \log \mathbb{E}\Big[H_l^{-2}\Big] - 2 \log \mathbb{E}\Big[H_l^{-1}\Big]. \quad (47)$$

The moments $\mathbb{E}[H_l^{-1}]$ and $\mathbb{E}[H_l^{-2}]$ can be evaluated through simulations, or numerically as

$$\mathbb{E}\Big[H_l^{-1}\Big] = \int_0^\infty \int_0^\infty (h_i + h_j)^{-1} f_{H_i}(h_i) f_{H_j}(h_j) dh_i dh_j,$$

$$\mathbb{E}\Big[H_l^{-2}\Big] = \int_0^\infty \int_0^\infty (h_i + h_j)^{-2} f_{H_i}(h_i) f_{H_j}(h_j) dh_i dh_j,$$

where $f_{H_1}(h_1)$ and $f_{H_2}(h_2)$ are the PDFs of H_i and H_j. Using the aforementioned properties, we obtain the CDF of $\Gamma_{(SD,s_1)}$ using (45) as

$$F_{\Gamma_{(SD,s_1)}}(y) = \frac{1}{2} \operatorname{erfc}\left(\frac{-\ln y + \mu^{CR}_{(SD,s_1)}}{\sqrt{2}\sigma^{CR}_{(SD,s_1)}} \right), \quad (48)$$

where $\mu^{CR}_{(SD,s_1)}$ and $\sigma^{SS}_{(SD,s_1)}$ are evaluated using (46) and (47), respectively. Similarly considering $\mathcal{D}$. The complementary CDF (CCDF) of the received SINR at D is given by

$$F_{\Gamma_{(SD,s_1)}}(y) = Pr\Big(\rho_S A^2_{SD}(d_{SD}, f) h^2_{SD} > y\Big), \quad (49)$$

$$= Pr\left(h^2_{SD} > \frac{y}{\rho_S A^2_{SD}(d_{SD}, f)}\right), \quad (50)$$

$$= Q\left(\frac{\ln(y) - \mu^{CR}_{(SD,s_1)}}{\sigma^{CR}_{(SD,s_1)}}\right). \quad (51)$$

$Q(.)$ represents the Gaussian Q-function, which is given as

$$Q(z) = \frac{1}{\sqrt{2\pi}} \int_z^\infty \exp\left(-\frac{b^2}{2}\right) db. \quad (52)$$

Subsequently, the expressions for $\mathcal{C}$ and $\mathcal{E}$ are obtained in the similar manner.

APPENDIX B
PROOF OF PROPOSITION 2

The outage for the symbol s_1 at D occurs when D fails to decode the symbol s_1 from the direct link or the cooperative link. That is given by equation (34), shown at the bottom of the p. 6 and we consider the first term in order to derive the analytical expressions. Since the random variables are i.i.d, (34) can be given as

$$P^{(CR)}_{\text{IHDAF}} \triangleq Pr\{\Gamma_{(SD,s_1)} \leq \alpha_1\} \times \Big(Pr\Big\{\Gamma_{(SD,s_1)} \leq \alpha_1, \Gamma^{DF}_{(SR,s_1)} > \alpha_1, \Gamma^{DF}_{(RD,s_1)} \leq \alpha_1\Big\} + Pr\Big\{\Gamma_{(SD,s_1)} \leq \alpha_1, \Gamma^{DF}_{(SR,s_1)} \leq \alpha_1, \Gamma^{AF}_{(RD,s_1)} \leq \alpha_1\Big\}\Big)$$

$$= F_{(SD,s_1)}(\alpha_1)\Big(F_{(SD,s_1)}(\alpha_1), \bar{F}^{DF}_{(SR,s_1)}(\alpha_1), F^{DF}_{(RD,s_1)}(\alpha_1) + F_{(SD,s_1)}(\alpha_1), F^{DF}_{(SR,s_1)}(\alpha_1), F^{AF}_{(RD,s_1)}(\alpha_1)\Big). \quad (53)$$

where $F_{(SD,s_1)}(\alpha_1)$, $F^{DF}_{(RD,s_1)}(\alpha_1)$, $F^{DF}_{(SR,s_1)}(\alpha_1)$ and $F^{AF}_{(RD,s_1)}(\alpha_1)$ denote the CDF of random variables $\Gamma_{(SD,s_1)}$, $\Gamma^{DF}_{(RD,s_1)}$, $\Gamma^{DF}_{(SR,s_1)}$ and $\Gamma^{AF}_{(RD,s_1)}$, respectively, evaluated at a point $\alpha_1 \in \mathbb{R}$. Moreover, $\bar{F}^{DF}_{(SR,s_1)}(\alpha_1) = 1 - F^{DF}_{(SR,s_1)}(\alpha_1)$. Rest of the proof follows by calculating these CDFs, by approximating the random variables $\Gamma_{(SD,s_1)}$, $\Gamma^{DF}_{(SR,s_1)}$, $\Gamma^{DF}_{(RD,s_1)}$ and $\Gamma^{AF}_{(RD,s_1)}$ as lognormal random variables with parameters obtained by following (46) and (47), as discussed in Appendix A. In particular, each of these lognormal parameters are calculated using the properties 1)-3) described in Appendix A. Substituting these parameters in the CDFs in (53) and further simplification gives the required result.

REFERENCES

[1] I. Mandourarakis, E. Koutroulis, and G. N. Karystinos, "Power line communication method for the simultaneous transmission of power and digital data by cascaded H-bridge converters," *IEEE Trans. Power Electron.*, vol. 37, no. 10, pp. 12793–12804, Oct. 2022.

[2] C. Cano, A. Pittolo, D. Malone, L. Lampe, A. M. Tonello, and A. G. Dabak, "State of the art in power line communications: From the applications to the medium," *IEEE J. Sel. Areas Commun.*, vol. 34, no. 7, pp. 1935–1952, Jul. 2016.

[3] N. Pavlidou, A. Han Vinck, J. Yazdani, and B. Honary, "Power line communications: State of the art and future trends," *IEEE Commun. Mag.*, vol. 41, no. 4, pp. 34–40, Apr. 2003.

[4] A. M. Tonello and A. Pittolo, "Considerations on narrowband and broadband power line communication for smart grids," in *Proc. SmartGridComm*, Nov. 2015, pp. 13–18.

[5] X. Cheng, R. Cao, and L. Yang, "Relay-aided amplify-and-forward powerline communications," *IEEE Trans. Smart Grid*, vol. 4, no. 1, pp. 265–272, Mar. 2013.

[6] A. M. Tonello and F. Versolatto, "New results on top-down and bottom-up statistical PLC channel modeling," in *Proc. 3rd Workshop Power Line Commun. Appl.*, Oct. 2009, pp. 11–14.

[7] G. López et al., "The role of power line communications in the smart grid revisited: Applications, challenges, and research initiatives," *IEEE Access*, vol. 7, pp. 117346–117368, 2019.

[8] H. Meng, Y. Guan, and S. Chen, "Modeling and analysis of noise effects on broadband power-line communications," *IEEE Trans. Power Del.*, vol. 20, no. 2, pp. 630–637, Apr. 2005.

[9] K. W. S. Palitharathna, H. A. Suraweera, R. I. Godaliyadda, V. R. Herath, and J. S. Thompson, "Average rate analysis of cooperative NOMA aided underwater optical wireless systems," *IEEE Open J. Commun. Soc.*, vol. 2, pp. 2292–2310, 2021.

[10] A. Samir, M. Elsayed, A. A. A. El-Banna, K. Wu, and B. M. ElHalawany, "Performance of NOMA-based dual-hop hybrid powerline-wireless communication systems," *IEEE Trans. Veh. Technol.*, vol. 71, no. 6, pp. 6548–6558, Jun. 2022.

[11] W. Duan, X.-Q. Jiang, M. Wen, J. Wang, and G. Zhang, "Two-stage superposed transmission for cooperative NOMA systems," *IEEE Access*, vol. 6, pp. 3920–3931, 2018.

[12] K. M. Rabie, B. Adebisi, E. H. G. Yousif, H. Gacanin, and A. M. Tonello, "A comparison between orthogonal and non-orthogonal multiple access in cooperative relaying power line communication systems," *IEEE Access*, vol. 5, pp. 10118–10129, 2017.

[13] K. M. Rabie, B. Adebisi, A. M. Tonello, S. Yarkan, and M. Ijaz, "Two-stage non-orthogonal multiple access over power line communication channels," *IEEE Access*, vol. 6, pp. 17368–17376, 2018.

[14] R. Ramesh, S. Gurugopinath, and S. Muhaidat, "Outage performance of relay-assisted single- and dual-stage NOMA over power line communications," *IEEE Access*, vol. 9, pp. 86358–86368, 2021.

[15] R. K. Ahiadormey, P. Anokye, H.-S. Jo, and K.-J. Lee, "Performance analysis of two-way relaying in cooperative power line communications," *IEEE Access*, vol. 7, pp. 97264–97280, 2019.

[16] W.-J. Li, N. Zhang, Z. Liu, J.-F. Wang, Y.-S. Guo, and D. Lv, "Information fusion method of power Internet of Things based on low-voltage power line and micro-power wireless communication," *IEEE Access*, vol. 10, pp. 89959–89969, 2022.

[17] S. Zhao, M. Tian, and Q. Li, "Robust transmission in non-orthogonal multiple access AF relay networks," *IEEE Wireless Commun. Lett.*, vol. 7, no. 6, pp. 1078–1081, Dec. 2018.

[18] M. Tian, S. Zhao, Q. Li, and J. Qin, "Secrecy sum rate optimization in nonorthogonal multiple access AF relay networks," *IEEE Syst. J.*, vol. 13, no. 3, pp. 2712–2715, Sep. 2019.

[19] A. Jee, K. Agrawal, and S. Prakriya, "A coordinated direct AF/DF relay-aided NOMA framework for low outage," *IEEE Trans. Commun.*, vol. 70, no. 3, pp. 1559–1579, Mar. 2022.

[20] Z. Fang, S. Shen, J. Liu, W. Ni, and A. Jamalipour, "New NOMA-based two-way relay networks," *IEEE Trans. Veh. Technol.*, vol. 69, no. 12, pp. 15314–15324, Dec. 2020.

[21] S. M. R. Islam, N. Avazov, O. A. Dobre, and K. Kwak, "Power-domain non-orthogonal multiple access (NOMA) in 5G systems: Potentials and challenges," *IEEE Commun. Surveys Tuts.*, vol. 19, no. 2, pp. 721–742, 2nd Quart., 2017.

[22] R. Ramesh and S. Gurugopinath, "Sum rate and outage performance of relay-aided NOMA over power line communication," in *Proc. SPCOM*, Aug. 2022, pp. 1–5.

[23] R. Ramesh and S. Gurugopinath, "Sum rate analysis of cooperative NOMA over dual-hop wireless-power line communication," in *Proc. INDICON*, Dec. 2021, pp. 1–6.

[24] Z. Wang and Z. Peng, "Secrecy performance analysis of relay selection in cooperative NOMA systems," *IEEE Access*, vol. 7, pp. 86274–86287, 2019.

[25] S. Singh and M. Bansal, "Performance analysis of NOMA-based AF cooperative overlay system with imperfect CSI and SIC," *IEEE Access*, vol. 9, pp. 40263–40273, 2021.

[26] R. Huang et al., "Performance analysis of NOMA-based cooperative networks with relay selection," *China Commun.*, vol. 17, no. 11, pp. 111–119, Nov. 2020.

[27] O. Abbasi, A. Ebrahimi, and N. Mokari, "NOMA inspired cooperative relaying system using an AF relay," *IEEE Wireless Commun. Lett.*, vol. 8, no. 1, pp. 261–264, Feb. 2019.

[28] Y. Liu, G. Pan, H. Zhang, and M. Song, "Hybrid decode-forward & amplify-forward relaying with non-orthogonal multiple access," *IEEE Access*, vol. 4, pp. 4912–4921, 2016.

[29] Y. Liu, Y. Liu, and G. Ma, "Hybrid decode-forward amplify-forward relaying with opportunistic layered multicast," in *Proc. WCSP*, Oct. 2018, pp. 1–7.

[30] Z. Bai, J. Jia, C.-X. Wang, and D. Yuan, "Performance analysis of SNR-based incremental hybrid decode-amplify-forward cooperative relaying protocol," *IEEE Trans. Commun.*, vol. 63, no. 6, pp. 2094–2106, Jun. 2015.

[31] S. Li, J. Liu, L. Bariah, S. Muhaidat, A. Wang, and J. Liang, "NOMA-based user cooperation with incremental hybrid forwarding protocols," *IEEE Open J. Commun. Soc.*, vol. 2, pp. 2536–2546, Nov. 2021.

[32] S. Efazati and P. Azmi, "Cross layer power allocation for selection relaying and incremental relaying protocols over single relay networks," *IEEE Trans. Wireless Commun.*, vol. 15, no. 7, pp. 4598–4610, Jul. 2016.

[33] K. M. Rabie, B. Adebisi, and H. Gacanin, "Outage probability and energy efficiency of DF relaying power line communication networks: Cooperative and non-cooperative," in *Proc. ICC*, May 2017, pp. 1–6.

[34] J. Zhang, L. Dai, R. Jiao, X. Li, and Y. Liu, "Performance analysis of relay assisted cooperative non-orthogonal multiple access systems," *IEEE Wireless Commun. Lett*, submitted to publication.

[35] D. Wang, Y. Song, and X. Wang, "Channel modeling of broadband powerline communications," in *Proc. ICCSN*, Dec. 2017, pp. 427–430.

[36] Y. Guo, Z. Yang, R. Huo, and Z. Xie, "Channel model for low voltage three-core power line communication," *IEEE Access*, vol. 7, pp. 154882–154888, 2019.

[37] S. Solanki, V. Singh, and P. K. Upadhyay, "RF energy harvesting in hybrid two-way relaying systems with hardware impairments," *IEEE Trans. Veh. Technol.*, vol. 68, no. 12, pp. 11792–11805, Dec. 2019.

[38] K.-S. Hwang, Y.-C. Ko, and M.-S. Alouini, "Performance analysis of incremental relaying with relay selection and adaptive modulation over non-identically distributed cooperative paths," in *Proc. IEEE Int. Symp. Inf. Theory*, Jul. 2008, pp. 2678–2682.

[39] J. C. S. Santos Filho, P. Cardieri, and M. D. Yacoub, "Simple accurate lognormal approximation to lognormal sums," *IEEE Power Electron. Lett.*, vol. 41, no. 18, pp. 1016–1017, Sep. 2005.

ROOPESH RAMESH (Member, IEEE) received the B.E. degree in electronics and communication engineering from the Dr. Ambedkar Institute of Technology, Visvesvaraya Technological University, Bengaluru, India, in 2016, and the M.Tech. degree in digital communication engineering from PES University, Bengaluru, in 2018. He is currently an Assistant Professor with the Department of Electronics and Communication Engineering, School of Engineering and Technology, CMR University. His current research interests include cooperative powerline communications, NOMA, and MIMO systems.

SANJEEV GURUGOPINATH (Senior Member, IEEE) is a Professor with the Department of Electronics and Communication Engineering, PES University, Bengaluru. His current research interests include beyond 5G communication systems, powerline communications, underwater acoustics, and speech signal processing. He was a co-recipient of the Best Paper Awards at IEEE INDICON 2016, IEEE ICEECCOT 2019, IEEE CONECCT 2020, IEEE CONECCT 2021, IEEE IEMECON 2021, and IEEE INDICON 2022.

SAMI MUHAIDAT (Senior Member, IEEE) received the Ph.D. degree in electrical and computer engineering from the University of Waterloo, Waterloo, in 2006. From 2007 to 2008, he was an NSERC Postdoctoral Fellow with the Department of Electrical and Computer Engineering, University of Toronto, Canada. From 2008 to 2012, he was an Assistant Professor with the School of Engineering Science, Simon Fraser University, Burnaby, BC, Canada. He is currently a Professor with Khalifa University and an Adjunct Professor with Carleton University, Canada. His research interests include advanced digital signal processing techniques for wireless communications, RIS, 5G and beyond, MIMO, optical communications, the IoT with emphasis on battery-free devices, and machine learning. He served as a Senior Editor and an Editor for the IEEE COMMUNICATIONS LETTERS, an Editor for the IEEE TRANSACTIONS ON COMMUNICATIONS, and an Associate Editor for the IEEE TRANSACTIONS ON VEHICULAR TECHNOLOGY. He is currently an Area Editor of the IEEE TRANSACTIONS ON COMMUNICATIONS and a Lead Guest Editor for the Special Issue on Large-Scale Wireless-Powered Networks With Backscatter Communications of the IEEE OPEN JOURNAL OF THE COMMUNICATIONS SOCIETY.